

NANOGRAIN WO₃ THIN FILMS AS ACTIVE LAYER FOR RESISTIVE TYPE GAS SENSORS

M. Stankova^{*}, X. Vilanova^a, J. Calderer^a, I. Gràcia^b, C. Cané^b, X. Correig

Department of Engineering Electronics, University Rovira i Virgili, Avda. Països Catalans 26, 43007 Tarragona, Spain

^aDepartment of Engineering Electronics, Polytechnic University of Catalonia, Barcelona, Spain

^bDepartment of Microsystems and Silicon Technologies, CNM, Bellaterra, Spain

Pure and Pt doped WO₃ thin films were studied as active layers for resistive type microhotplate gas sensors. The layer of WO₃ was deposited by reactive rf magnetron sputtering on four element micromachined sensor array and was defined using lift-off method. The obtained film was doped with Pt employing the same deposition technique. An annealing process at 400 °C for 2 h in air was realized to ensure the film stability. The morphology of the layer was studied by SEM. Transmission electron microscopy was used to analyse the platinum thickness and distribution. The WO₃ phase was determined by XRD. The obtained sensors were used to detect traces of pollutants in a carbon dioxide stream. The results showed that the sensors were capable to detect the sulphur compounds in the presence of hydrocarbons. The pure WO₃ sensors were sensitive to very low concentrations of H₂S (100 ppb), while the doped ones presented high response to 1 ppm of SO₂. The influence of the operating temperature and the electrodes configuration was also studied.

(Received April 18, 2005; accepted May 26, 2005)

Keywords: WO₃; thin film gas sensors, Rf sputtering, CO₂ quality

1. Introduction

Nowadays, there is an increasing social concern about the quality and safety of foodstuffs, which has led to food industry associations and/or governments to establish quality and safety standards. This is what the beverage industry has done with the quality of CO₂, for which the International Society of Beverage Technologists (ISBT) has established quality guidelines [1]. The carbon dioxide is one of the main components of many of the beverages produced today, including soda, beer, sparkling water, and sport drinks. The procedures employed in the production of carbon dioxide involve such pollutants as oxygen, hydrocarbons (e.g. methane, ethylene, BTX compounds) and sulphur compounds (e.g. sulphur dioxide and hydrogen sulphide) which may be present at trace levels.

Many commercial analysers are available to control the CO₂ quality. Among them, the more used are based on gas chromatography and mass spectroscopy [2]. The inconvenience is that these equipments are expensive, volumetric and require a qualified personal. That is why, a low-cost, small size, portable analyser will be of great interest. In this context, the use of an array of metal oxide gas sensors could be an appropriate solution.

It is well known that the primary mechanism responsible for gas detection with metal oxide semiconductors in air at elevated temperatures is the change in the concentration of adsorbed oxygen at the semiconductor [3]. Nevertheless, in the last years several authors have reported on detection in inert gases such as argon [4] and nitrogen [5]. In this context, Vilanova *et al.* [6] developed a system of tin dioxide based sensors doped with different materials to detect traces of ethylene, methane and sulphur dioxide in CO₂ stream. However, their sensors showed low sensitivity to sulphur

* Corresponding author: mariana.stefanova@urv.net

compounds. For that reason, to improve the capability of the analyser, we developed sensors based on pure and Pt doped WO_3 . Tungsten trioxide was chosen as active material because it was demonstrated that it exhibits a good sensitivity to hydrogen sulphide [7-10] and sulphur dioxide [11] in air. We opted for micromachined sensor substrate because of the advantages that this presents. The sensitive layer of micromachined metal oxide gas sensors is deposited onto a thin dielectric membrane of low thermal conductivity, which provides good thermal isolation between substrate and the gas-sensitive heated area on the membrane. In this way the power consumption can be kept very low (typical values lie between 30 and 150 mW [12-14]) and the substrate itself stays nearly at ambient temperature.

2. Experimental

2.1. Substrate fabrication

An array of four microsensors elements was fabricated on p-type $\langle 1\ 0\ 0 \rangle$ silicon substrate. First, a membrane layer consisting of 0.3 μm -thick Si_3N_4 layer was growth by LPCVD. Next, a POCl_3 -doped polysilicon heater of 6 Ω/\square and 0.47 μm was deposited and patterned. The heater was used also as temperature sensor. A 0.8 μm -thick SiO_2 film was deposited as insulation layer between the heater and the electrodes made of sputtered Pt (0.2 μm) and patterned by lift-off. Two different configurations of interdigitated electrodes were used (with interelectrode gap of 50 and 100 μm ; see Fig. 1). The electrode area was 400 \times 400 μm and the membrane size was 1 \times 1 mm.

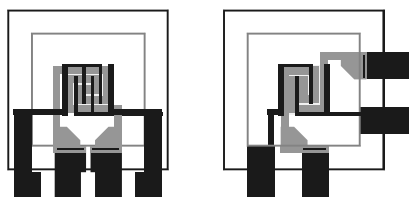


Fig. 1. Planar view of the different electrode configuration. Left- with 50 μm gap; right- with 100 μm gap.

In the next step the backside mask was patterned. Following, the active layer was deposited (the process is described in the next part). Silicon micromachining from the backside was carried out with KOH at 70 $^\circ\text{C}$. Finally, the sensors were bonded and packaged.

2.2. Active layer deposition

An active layer of tungsten trioxide was deposited by reactive rf magnetron sputtering. The used target was W (99.95 % of purity) with a diameter of 100 mm and thickness of 0.125 inches. The target substrate distance was fixed at 70 mm. The deposition was performed at room temperature. Argon was used as carrier gas and oxygen as reactive gas. By separate flowmeters the ratio $\text{Ar}:\text{O}_2$ was controlled to 50%:50%. The rf forward input power was maintained at 200 W with zero reflected power. The deposition process took 2 h. Half of the wafer was doped with Pt. For the dopant deposition, the same technique of rf sputtering was applied. For this purpose a Pt target (99.99 % of purity) was used. The deposition temperature and the target distance were remained unchanged. The sputtering atmosphere for this second deposition consisted just of Ar. The rf power was maintained at 50 W with zero reflected power. This deposition took 10 s. Both WO_3 and Pt were defined by lift-off process. Finally, the devices were annealed at 400 $^\circ\text{C}$ for 2 h in dry air.

2.3. Active layer characterization

The morphology of the layer was studied by SEM. The used microscope was Joel JSM 6400 with resolution of 0.3 nm and magnification from 15 to 300k. Before introducing the sample in the equipment, it was coated with a thin gold film to avoid charging effects. Transmission electron microscopy was used to observe the distribution of the doping material and to measure the thickness of the Pt layer. For this study a Pt doped WO_3 was deposited directly on Si wafer and annealed for

2 h at 400 °C. This was undertaken because of the impossibility to make the preparation of the micromachined sample for TEM analysis (because of the rupture of the membrane). The used equipment was Hitachi H-800-MT microscope with Gatan Multiscan camera, working at 200 kV. The TEM has magnification from 200 to 500k and resolution of 0.3 nm. To obtain the WO₃ phase structure, a XRD was carried out. XRD measurements were made using a Siemens D5000 diffractometer (Bragg-Brentano parafofocusing geometry and vertical θ - θ goniometer) fitted with a grazing incidence (ω : 0.52°) attachment for thin film analysis and scintillation counter as a detector. The angular 2θ diffraction range was between 21.0 and 70.0°. The data were collected with an angular step of 0.05° at 3 s per step and sample rotation. Cu_{K α} radiation was obtained from a copper X-ray tube operated at 40 kV and 30 mA.

2.4. Gas sensitivity measurements

To characterize the gas sensing properties two arrays (one of pure and one of doped WO₃ sensors) were connected in a thermally controlled chamber (16 cm³ of volume). Each array consisted of four sensors (two with 50 μ m gap and two with 100 μ m gap). First, pure CO₂ flowed through the chamber and the sensor base line was established. Then the flow, set to 90 ml/min, was swapped to CO₂ with a given pollutant (from a calibrated bottle), and the sensor resistances were acquired. Table 1 summarises the pollutants measured and their concentrations in CO₂ as balance gas.

Table 1. Studied gases and concentrations

Pollutant	Concentration
Sulphur dioxide	1 ppm
Hydrogen sulphide	100 ppb
Methane	30 ppm
Ethylene	20 ppm

The sensors were operated at 110, 200 and 380 °C for devices with interelectrode gap of 50 μ m and 150, 250 and 480 °C for those with gap of 100 μ m. Differences in the operating temperatures are due to the fact that the membranes with different electrode gap had different values of the heaters (550 and 650 Ω for 50 and 100 μ m gap, respectively) and the same current was applied to them. Each pollutant was measured at the three temperatures considered and each measurement was replicated five times.

3. Results and discussion

3.1. Structural characterization

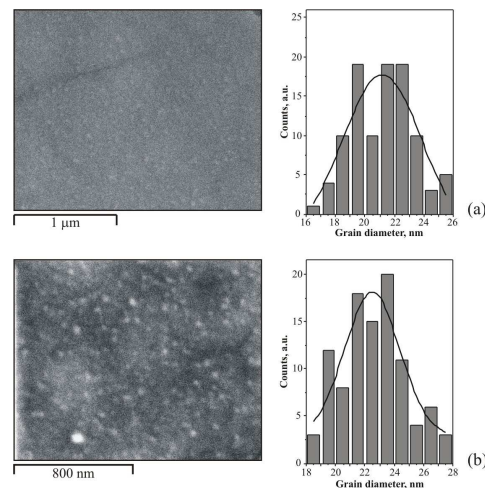


Fig. 2. SEM image of: (a) pure WO₃; (b) WO₃ doped with Pt

Fig. 2 shows the morphology of the pure and Pt doped layer after the annealing process. From the figure it can be observed that the mean grain diameter for the pure layer (21.101 ± 2.028 nm) is a little bit smaller than that for the doped layer (22.53 ± 2.136 nm). Both sizes can be considered as equal, which fact suggests that the platinum deposited on the surface does not promote the agglomeration.

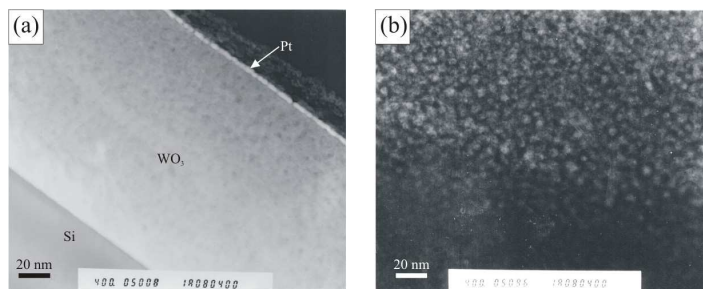


Fig. 3. TEM images of WO_3/Pt layer. (a) a cross-section sample; (b) a plane sample

By the means of TEM two samples were studied (a cross-section and a plane). From the first of them we obtained the thickness of the platinum layer (fig. 3a). The film was superficial and 3-4 nm thick. From the second, the platinum distribution can be observed (see fig. 3b). The dopant film was uniform with mean grain diameter of 2.636 ± 0.387 nm. It can be seen that this value is very closed to the thickness of the layer.

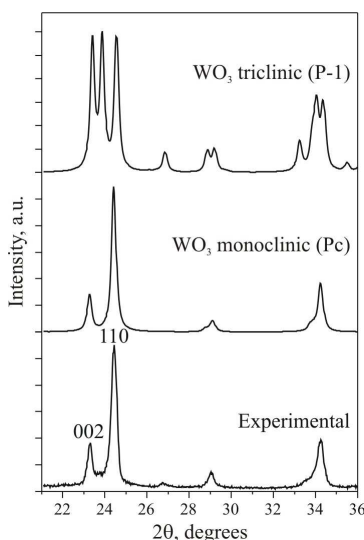


Fig. 4. XRD spectrum for WO_3 . The diffractograms for monoclinic (Pc) and triclinic (P-1) are shown for comparison.

The phase composition of the WO_3 was obtained by XRD. The result of this analysis is shown in figure 4. The peaks labelled on this figure correspond to monoclinic (Pc) tungsten oxide. However, some of the peaks characteristic of the monoclinic phase are absent and other peaks, which are characteristic of triclinic (P-1) WO_3 , are present. This allows us to conclude that the main phase of the tungsten oxide is the monoclinic one, but some triclinic tungsten oxide coexists.

3.2. Gas sensing properties

The capability of the sensors to detect pollution of CO₂ by hydrocarbons and sulphur compounds was studied. The results obtained showed that the sensors were almost insensitive to methane and ethylene. On the other hand, they presented very good responses to H₂S and SO₂. Particularly, pure WO₃ sensor was very sensitive to H₂S, but not to SO₂, while the doped devices had the opposite behaviour. Moreover, when the flow is returned to pure CO₂, the sensors recovered their initial resistance value, which proves the reversibility of the sensing mechanism for these pollutants in CO₂.

To study the effect of the operating temperature and the electrode geometry, the sensor response was defined as $|R_g - R_a|/R_x$, where R_a is the base line resistance in pure CO₂ and R_g is the sensor resistance in presence of the polluted carbon dioxide. The term R_x corresponds to R_a for oxidizing gases (SO₂ in this case), while for reducing gases (the case of H₂S) corresponds to R_g . The results (the average for five measurements) are shown in Fig. 5.

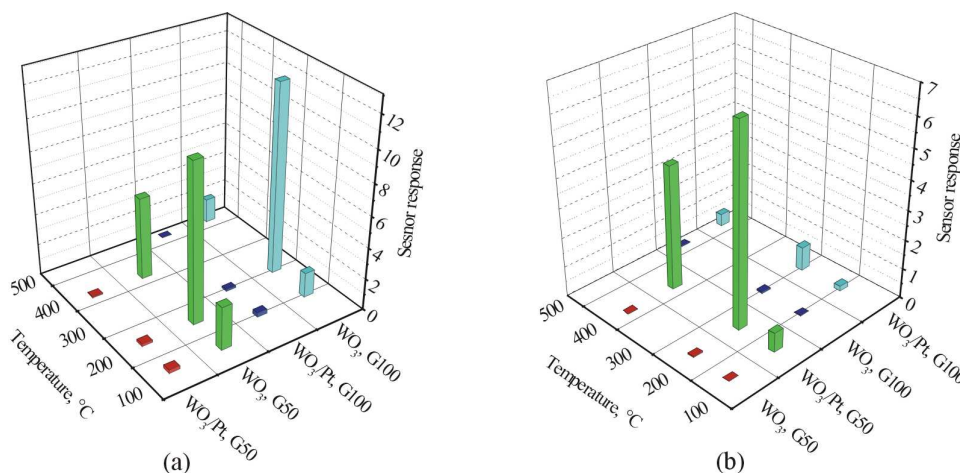


Fig. 5. Dependence of the sensor response on the operating temperature. (a) for H₂S. (b) for SO₂. Labels G50 y G100 denote inter-electrode gap of 50 and 100 μm, respectively.

Fig. 5(a) shows that the doped sensor are almost insensitive to H₂S, although the response decreases when the temperatures increases. On the other hand, the pure tungsten trioxide sensor shows high responsivity to this gas with a maximum response at the intermediate temperature (200 °C for electrodes with 50 μm gap and 250 °C for electrodes with 100 μm gap). In this unique case the electrode geometry has no clear effect in the response, while for the other two working temperatures the devices with 50 μm gap electrodes present higher response than the ones with 100 μm gap electrodes. This result is logical and is in accordance with the theory of the electrode geometry, which predicts an increase in sensor response if electrode spacing is reduced and film thickness and electrode length are kept unchanged [15].

Figure 5(b) shows a high response for SO₂ of the doped sensors, while the pure ones show very low responsiveness to this contaminant for all the temperatures considered. The response of the doped sensors to the sulphur dioxide reaches a maximum at intermediate temperatures (200 °C for the sensors with 50 μm electrode gap and 250 °C for the sensors with 100 μm electrode gap). Comparing the results for the pure and doped devices, it can be seen that the behaviour with temperature is the same for both types of electrodes. Nevertheless, the response for devices with 50 μm gap is higher than for the ones with 100 μm gap.

All these results show that an array of two sensors with 50 μm gap electrodes (composed by one Pt doped and one pure WO₃) working at 200 °C, can be used to monitor the quality of CO₂ for beverage industries and detect the pollution by sulphur compounds (SO₂ and H₂S). The results also prove that the presence of hydrocarbons (as methane or ethylene) will not affect this capability. Nevertheless, the possible interference of nitrogen oxides or ammonia must be considered and analysed, since WO₃ has shown good sensitivities for these gases in air.

4. Conclusions

A micromachined sensor array has been fabricated. Pure and Pt doped WO_3 deposited by rf magnetron sputtering has been used as sensing layer. The morphology of the films has been studied by SEM. The layers show a polycrystalline structure formed by grains with average diameters of the order of 21-22 nm. By TEM, the mean grain diameter of the Pt was obtained (about 3 nm). Using XRD it was found that the WO_3 was mainly present in monoclinic phase, although triclinic phase coexisted.

The capability of pure and Pt doped WO_3 to detect the presence of sulphur compounds as pollutants in CO_2 has been investigated. The sensors have shown high and reversible responses to the presence of H_2S and SO_2 diluted in CO_2 , in absence of oxygen (concentration below 15 ppm). The intrinsic sensors presented very good response to H_2S (100 ppb in CO_2) and poor response to SO_2 (1 ppm in CO_2), while the doped ones showed a reversed behaviour. Besides, H_2S behaves as a reducing gas (decreasing sensor resistance), while SO_2 behaves as an oxidizing species (increasing sensor resistance). The best results have been obtained for an operating temperature around 200 °C. Taking into account these results, an array combining these two active layers is a promising system to detect the CO_2 pollution by sulphur compounds. Nevertheless, the probable interference of other gases as ammonia or nitrogen oxides has to be analyzed to assure this application, since WO_3 has been proved to be very sensitive to these gases in air.

In order to optimize the sensors geometry, an analysis of the influence of the parameters on the sensor behaviour was studied. The results obtained state that interdigitated electrodes with smaller gap show, in general, better performance than the ones with larger gap. So the first type of electrodes is preferred for further studies and sensor development.

References

- [1] ISBT carbon dioxide quality guidelines and analytical procedure bibliography, International Society of Beverage Technologists, USA, March 2001.
- [2] R. L. Firor, B. D. Quimby, Agilent Technologies Inc., USA, April 2, 2001.
- [3] S. R. Morrison, in *Semiconductor sensors*, Ed. S. M. Sze, Wiley, USA, 1994, p. 383.
- [4] L. F. Reyes, S. Saukko, A. Hoel, V. Lantto, C. G. Granqvist, *J. Eur. Ceram. Soc.* **24**, 1415 (2004).
- [5] W. Schmid, N. Bârsan, U. Weimar, *Sens. Actuators B* **103**, 362 (2004).
- [6] X. Vilanova, X. Correig, E. Llobet, J. Brezmes, R. Calavia, X. Sánchez, Spanish Patent ES2212739, Priority date 2003.
- [7] B. Frühberger, M. Grunze, D. J. Dwyer, *Sens. Actuators B* **31**, 167 (1996).
- [8] E. P. S. Barrett, G. C. Georgiades, P.-A. Sermon, *Sens. Actuators B* **1**, 116 (1990).
- [9] J. L. Solis, S. Saukko, L. B. Kish, C. G. Granqvist, L. Lantto, *Sens. Actuators B* **77**, 316 (2001).
- [10] W.-H. Tao, C.-H. Tsai, *Sens. Actuators B* **81**, 237 (2002).
- [11] Y. Shimizu, N. Matsunaga, T. Hyoto, M. Egashira, *Sens. Actuators B* **77**, 35 (2001).
- [12] S. Fung, Z. Tang, P. Chan, J. Sin, P. Cheung, *Sens. Actuators A* **54**, 482 (1996).
- [13] A. Götz, I. Gràcia, C. Cané, E. Lora-Tamayo, *J. Micromach. Microeng.* **7**, 247 (1997).
- [14] M. Stankova, P. Ivanov, E. Llobet, J. Brezmes, X. Vilanova, I. Gràcia, C. Cané, J. Hubalek, K. Malysz, X. Correig, *Sens. Actuators B* **103**, 23 (2004).
- [15] J. W. Gardner, *Sens. Actuators B* **1**, 166 (1990).